An Ultrawideband All-Textile Metamaterial Absorber for Ku-, K-, and Ka-Band Applications

Esra Celenk, *Member, IEEE*, Charles Lynch, *Student Member, IEEE*, and Manos M. Tentzeris, *Fellow, IEEE*

***Abstract*—An all-textile metamaterial absorber is proposed for Ku-, K-, and Ka-band applications. The proposed metamaterial absorber is based on square-shaped split ring resonators. The design parameters are chosen based on commonly used electronic textile (E-textile) and felt dielectric material. The proposed structure demonstrates has a high absorption property of >90% between 13.1 and 31.13 GHz. At the same time, it reaches 99% absorption value between 16.4 and 21 GHz. The textile metamaterial absorber features the advantages of ultrawideband operability, angular stability, and polarization insensitivity. A proof-of-concept all-textile metamaterial absorber prototype has been fabricated and its simulation performance has been confirmed successfully by measurements. The results obtained are promising for the development of E-textile-based applications, such as energy harvesting, camouflage systems, sensitive wearable electronics, health monitoring, and electromagnetic shielding.**

***Index Terms*—Metamaterial, textile absorber, textile metamaterial, wideband absorber.**

I. Introduction

SMART textiles are fabrics that offer integrated electronic functionality on a textile structure, unlike normal textile fabrics [1]. Smart textile technology has dramatically evolved over last decade, especially in the area of electronic textiles (E-textile) featuring conductive properties. Smart textile applications are very diverse and used many wide application range encompassing health services, medical monitoring, personal tracking, military purposes, and radar applications [2].

E-textile studies should be robust, reliable, and compact for different conditions, as well as cost-effective [3].

In general, in E-textile designs, conductivity is enabled by conductive fabrics. Nonconductive fabrics, such as silk, wool, leather, polyester, or felt are used as dielectric materials [4], [5].

Although battery integration with E-textiles has been challenging, numerous energy harvesting solutions have been introduced using ambient radio waves, solar energy, human body movements, and human body heat. Metamaterial-based E-textile applications have been also gathering significantly increased interest solution methods. Considering the low power requirement, smart textiles are candidates to be strengthened by energy harvesting techniques as in [6]. Thus, less bulky systems with or without batteries can be obtained [7]. Collecting energy from radio frequency sources or human bodies to meet battery needs can be an alternative source for low-power systems and smart textile applications. Metamaterial-based absorbers are one of the recommended solutions with their features, such as high absorber efficiency [8], [9].

Metamaterial absorbers have been studied and applied in a wide variety of fields, from microwaves to optical frequencies, featuring robust performance independent of angular variation and polarization, proving they can be very good solution for systems. The usage of metamaterial absorbers is an alternative to the development of systems with high absorption requirements [10].

Frequency selective surfaces (FSS) can be used for the implementation of electromagnetic metamaterial absorbers, typically in the form of sandwich configurations, where a nonconductive substrate is placed between the conductive patch with a periodic pattern and the conductive ground plane at the top [11]. FSS-based electromagnetic structures pass or block selected frequency bands of electromagnetic waves according to their size and shape. In addition, the amplitude, phase, and polarization of electromagnetic waves can be controlled with metamaterials [12], [13].

In this letter, an all textile metamaterial absorber operating in the ultrawideband between 13.1 and 31.13 GHz is proposed. The proposed structure includes Ku-, K-, and Ka-band operating frequencies. At the same time, the presented all-textile topology is insensitive to polarization. In the design of a proof-of-concept prototype E-textiles were used for the conductive layers and wool felt as the dielectric material. Simulation and experimental results show features excellent (absorption $> 90\%$) ultrabroadband absorption properties.

II. Proposed Metamaterial Absorber Unit Cell Design and Characteristics

Fig. 1 shows the geometry of the unit cell of the proposed metamaterial absorber, that consists of three layers. The upper layer and the ground layer are E-textile. The surface resistivity of the used E-textile is less than 0.05 Ω/sq [14]. The felt, which is used as the sandwiched dielectric layer has the properties of $\varepsilon_r = 1.4$ and $\tan\delta = 0.02$ [15]. The unit cell of the metamaterial absorber is inspired from split-ring resonators with the thicknesses of the felt dielectric and E-textile conductor to be 3 and 0.06 mm, respectively. The detailed parameter dimensions of the metamaterial absorber unit cell is given in Table I.

Manuscript received 14 December 2023; revised 9 February 2024; accepted 21 February 2024. Date of publication 26 February 2024; date of current version 4 June 2024. *(Corresponding author: Esra Celenk.)*

The authors are with the School of Electrical and Computer Engineering, Georgia Institute of Technology, Atlanta, GA 30332 USA (e-mail: esra.celenk@ece.gatech.edu; clynch42@gatech.edu; etentze@ece.gatech.edu).

Digital Object Identifier 10.1109/LAWP.2024.3369971

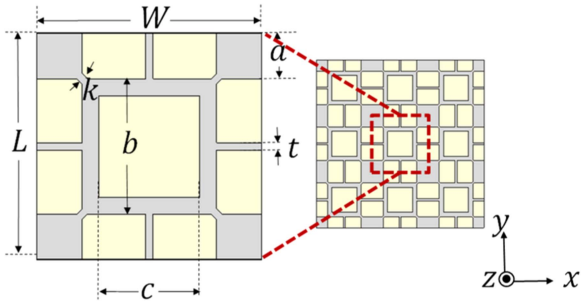

Fig. 1. Schematic of the all-textile metamaterial absorber unit cell. Gray areas are conductive, whereas straw-colored regions are dielectric (felt).

TABLE I
DIMENSIONS AND PARAMETERS OF THE PROPOSED METAMATERIAL ABSORBER UNIT CELL

Parameter	Value (mm)	Parameter	Value (mm)
W	60	c	21
L	60	k	3
a	12	t	3
b	36		

All values in Table I were obtained as a result of parametric analysis in the full-wave software CST. The length k is critical for the spacing of the squares in the corners of the textile unit cell that are placed around the center resonator, while preventing the conductive textile from breaking during production or bending.

The k values between 1 and 3 mm connecting the square ring resonator in the middle and the square resonators at the corners have no effect on the bandwidth and the absorption. The purpose of the thickness k is to ensure that the parts do not break from each other during the production of the textile work. As the square ring resonator width (c) in the middle of the unit cell decreases, the bandwidth does not change, but the absorption increases significantly. The width of the conductive strip extending from the middle resonator to the unit cell edge does not affect the bandwidth, while increasing its value leads to lower absorption. However, increasing the value t decreases the absorption. The felt thickness used in the design has a very important effect on both absorption and bandwidth. Increasing the felt thickness reduces the bandwidth.

The simulated variation of the reflection coefficient values of the proposed all-textile metamaterial unit cell absorber as a function of frequency is plotted in Fig. 2. Resonance is observed at 17.9 GHz. The designed metamaterial unit cell has a bandwidth of 18.03 GHz covering all frequencies between 13.1 and 31.13 GHz.

The metamaterial absorber unit cell was simulated with periodic boundary conditions and Floquet-port excitations using full-wave software CST. In addition, appropriate unit cell boundary conditions were used to observe the transverse electric (TE) and transverse magnetic (TM) incident wave cases

$$A(\omega) = 1 - R(\omega) - T(\omega) = 1 - |S_{11}|^2 - |S_{21}|^2. \quad (1)$$

The absorption efficiency can be calculated using (1), where $R(\omega)$ and $T(\omega)$ represent the amount of power reflected and transmitted, respectively, that are effectively correlated to the S_{11} and S_{21} (scattering parameters) [16], [17], [18].

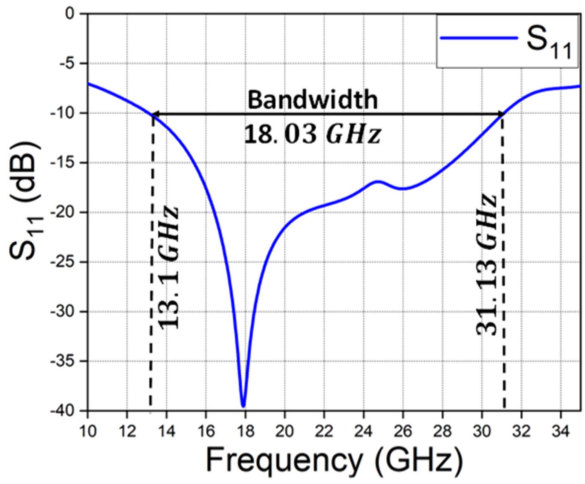

Fig. 2. Reflection coefficient variation versus frequencies of all-textile metamaterial absorber.

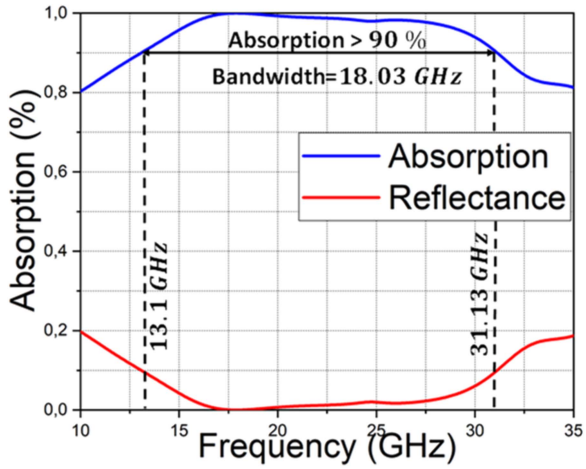

Fig. 3. Absorption and reflectance diagram of all-textile metamaterial absorber.

The absorption and reflectance diagram of the metamaterial unit cell absorber is given in Fig. 3. As can be seen in the figure, the designed metamaterial unit cell features over 90% absorption between 13.1 and 31.13 GHz (bandwidth of 18.03 GHz) with 99% absorption from 16.4 to 21 GHz. It shows over 95% absorption at over a 14.85 GHz bandwidth. As seen in Fig. 3, the metamaterial absorber reaches 99% absorption between 16.4 and 21 GHz.

The value of the unit cell equivalent normalized impedance can be determined by using the phase and amplitude of electromagnetic waves transmitted and reflected from the all-textile structure and can be calculated by [18], [19]

$$Z = \pm\sqrt{\frac{(1+S_{11})^2 - S_{21}^2}{(1-S_{11})^2 - S_{21}^2}}. \quad (2)$$

Reflection is suppressed when the equivalent impedance of the device and the free space impedance are fully matched. In this case, Re[Z] = 1 and Im[Z] = 0. Also, the absorption rate reaches

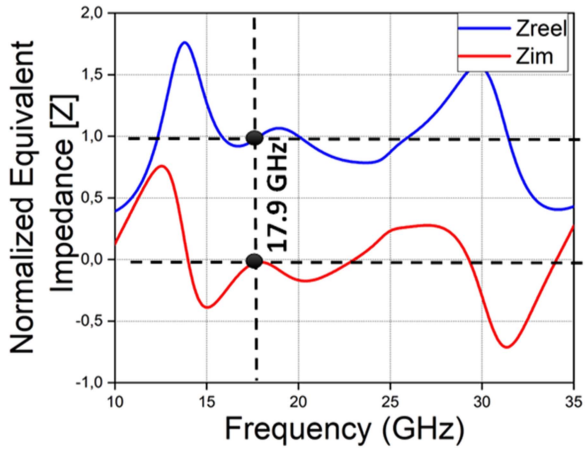

Fig. 4. Normalized equivalent impedance diagram of all-textile metamaterial absorber.

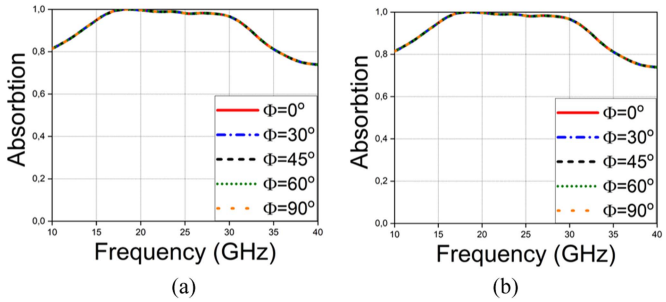

Fig. 5. Absorption characteristic of all-textile metamaterial absorber with different polarization angles. (a) TE polarization. (b) TM polarization.

its maximum value as seen Fig. 4. The real part of the impedance is around 1, and the imaginary part is around 0 between 13.1 and 31.13 GHz. It is seen that the imaginary part of the equivalent impedance is equal to 0 and the real part is equal to 1 at the resonant frequency of 17.9 GHz. The absorption value is about 99.98% in resonance value.

The polarization insensitivity of the proposed all textile metamaterial absorber was investigated for TE and TM polarizations between 0° and 90°. The response of the structure to different polarization angles (Φ) is shown in Fig. 5. Simulation results show that this proposed absorber has above 90% absorption bandwidth from 13.1 to 31.13 GHz with angular stability in the Ku-, K-, and Ka-band. The polarization insensitivity of the proposed structure is directly related to the symmetrical geometric structure of the upper E-textile design.

In addition to polarization insensitivity, the absorption effect of the structure should be investigated at different oblique incidence angle situations. Therefore, the proposed metamaterial absorber structure impact of different oblique incident angle θ $(0^\circ - 45^\circ)$ was studied for TE and TM polarizations, and the results are shown in Fig. 6. It can be clearly seen from Fig. 6 that the absorption value change for TE and TM polarization at different oblique incidence angles is very small. Therefore, the absorption characteristic dependence of the proposed metamaterial absorber on the incident angle is also negligible. While examining the absorption behavior of the all-textile metamaterial

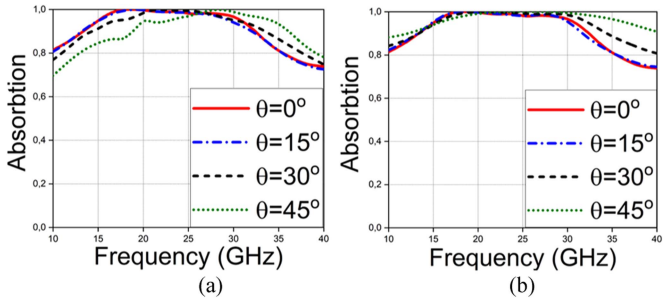

Fig. 6. Absorption characteristic of all-textile metamaterial absorber with different oblique incident angle for (a) TE polarization and (b) TM polarization.

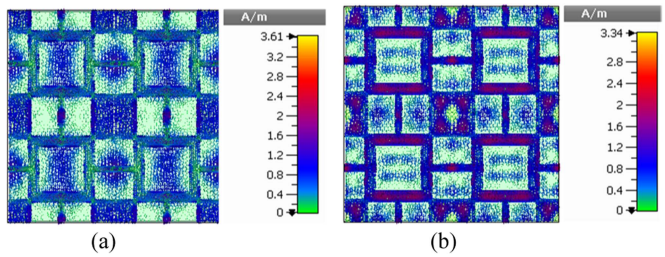

Fig. 7. Surface current distributions for the all-textile metamaterial absorber at (a) $f_1 = 13.1$ GHz and (b) $f_2 = 31.13$ GHz.

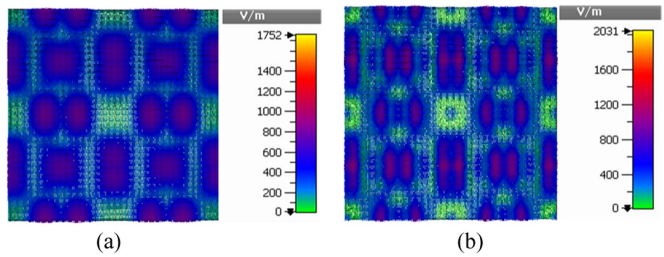

Fig. 8. Electric field distributions for the all -textile metamaterial absorber at (a) $f_1 = 13.1$ GHz and (b) $f_2 = 31.13$ GHz.

absorber structure under the TE polarization state, the propagation direction of the electromagnetic wave and the direction of the magnetic field rotate at different oblique angles of incidence (θ), while the electric field direction remains unchanged. In the case of TM polarization, the propagation direction of the electric field and the incoming electromagnetic wave rotates at different oblique angles of incidence, while the direction of the magnetic field remains unchanged [20]. For TE and TM polarization cases, it is observed that the all-textile absorber structure offers more than 80% absorption capability up to 45° oblique incidence angle between 13.1 and 31.13 GHz.

The wideband absorber property of the proposed metamaterial absorber is investigated. In addition, the electric field distribution at the surface of the conductor and surface electric current of the structure are also investigated. The examination is carried out at the high frequency value and the low frequency value, where the structure showed an absorption of more than 90% and shown in Figs. 7 and 8, respectively.

As can be seen in Fig. 7(b), as the frequency increases according to the surface current distributions, the surface currents are formed around larger square resonators. As shown in Fig. 8,

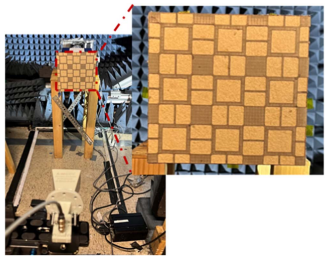

Fig. 9. Fabricated prototype of the all-textile metamaterial absorber.

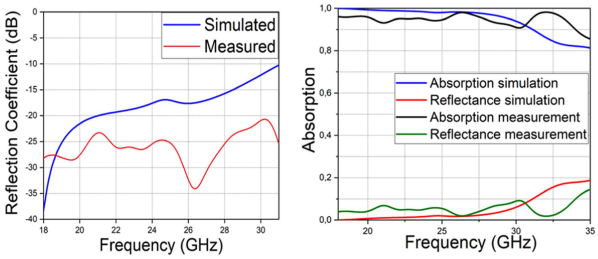

Fig. 10. (a) Measured reflection coefficient. (b) Measured absorption and reflectance diagram of the all-textile metamaterial absorber.

TABLE II
COMPARISON OF THE PROPOSED ABSORBER PERFORMANCE WITH EXISTING PUBLISHED ALL-TEXTILE METAMATERIAL ABSORBER STRUCTURES

Ref	Operating frequency (absorption > 90%)	Bandwidth (absorption >90%)	Angular Stability (Φ)*	Material
[11]	9 GHz - 9.8 GHz	Narrow bandwidth	0°-90°	Felt, E-textile
[17]	10.64 GHz	Narrow bandwidth	Not given	Cotton, Conductive yarn
[21]	7.39 GHz – 18 GHz	10.61 GHz	Not given	PWC[a]/ TWC[b], Resistive inks
[22]	9.75 GHz - 10.08 GHz	0.33 GHz	0°-90°	Fabrics[c], Conductive paint
This work	13.1 GHz - 31.13 GHz	18.03 GHz	0°-90°	Felt, E-textile

*Simulation results
[a]PWC =Plain weave cloth, [b]TWC=Twill weave cloth
[c]Fabrics= Weft-knitted and plain weave fabric

most of the electric field in the low frequency and high frequency value in the proposed metamaterial absorber broadband appears to be concentrated in the frame line located in the middle of the design.

III. Fabrication and Experimental Verification

Metamaterial absorber is produced from wool felt and E-textile materials. The E-textile material is 0.06 mm thick and is resistant to temperatures up to 200 °C [12]. The production of metamaterial absorbers, which are all textiles, begins with the determination of the boundary lines of the design and cutting with a laser machine. Thanks to laser cutting, the fuzz that may occur on the felt edges is almost eliminated. The self-adhesive of E-textile, which is used as a conductive material, not only simplifies production, but also reduces potential losses. Usage of standard textile fabrication techniques enables simple and cost-effective mass production of the proposed absorber. To verify the all-textile metamaterial absorption of the designed absorber experimentally, textile sample of size 180 mm × 180 mm were fabricated, as shown in Fig. 9. A pair of horn antenna working in 18–40 GHz was used for testing. Anritsu MS46522B two-port vector network is used in measurements. The result of the reflection coefficient in the working range of the antenna used in the measurement is given in Fig. 10(a). As can be seen in Fig. 10(a), a good agreement was obtained between the simulated and measured results between 18 and 31 GHz.

Measured absorption and reflectance diagram of all textile metamaterial absorber is given as the function of frequency in Fig. 10(b) together with the simulated results. Since the operating frequency of the measured reference horn antenna starts from 18 GHz, Fig. 10(b) shows frequencies of 18–35 GHz.

According to the simulation results, the antenna, which has an absorption feature of over 90% up to 31.13 GHz, shows an excellent absorption feature of over 90% up to 34 GHz in the measurement results. The shift in frequency is thought to be caused by measurement and production errors. As can be seen in Fig. 10(b), the measured ultrawideband all textile metamaterial absorber shows excellent absorbency of approximately 95% in the 18–34 GHz range. The measured reflectance of the all-textile metamaterial absorber value is very suitable with the simulation result and is below 0.1 between 18 and 34 GHz. A comparison of the proposed absorber performance with all existing textile metamaterial studies is given in Table II. The table has been prepared according to the simulation and measurement results of the studies. As given in Table II, all the proposed textile metamaterial absorber study has an ultrawideband feature between 13.1 and 31.13 GHz and exhibits over 90% absorber properties in this band. This situation is supported by the measurement result. The proposed absorber is also insensitive to different polarization angles between 0° and 90°.

V. Conclusion

In this letter, an ultrawideband all textile metamaterial absorber has been presented. A square split ring resonator like shaped metamaterial unit cell is used in order to obtain ultrawideband absorption between 13.1 and 31.13 GHz. This design has high absorption (>90%) with a bandwidth of 18.03 GHz, which includes some of the Ku-, K-, and Ka-bands. The all textile metamaterial absorption efficiency is over 99% at 16.4 and 21 GHz bandwidth. Moreover, the textile metamaterial absorber has an angular stability (90°) and polarization insensitivity for various angular incidences. The design, which can be measured between 18 and 40 GHz, is perfectly compatible with the simulation result in this frequency range. According to the measurement result, the absorption performance of the proposed design in 18 and 34 GHz bandwidth is approximately 95%.

REFERENCES

[1] M. Stoppa and A. Chiolerio, "Wearable electronics and smart textiles: A critical review," *Sensors*, vol. 14, no. 7, pp. 11957–11992, 2014.

[2] A. Komolafe et al., "E-textile technology review-from materials to application," *IEEE Access*, vol. 9, pp. 97152–97179, 2021.

[3] J. Kubicek et al., "Recent trends, construction, and applications of smart textiles and clothing for monitoring of health activity: A comprehensive multidisciplinary review," *IEEE Rev. Biomed. Eng.*, vol. 15, pp. 36–60, 2022.

[4] E. Celenk and N. T. Tokan, "All-textile on-body metasurface antenna," *Prog. Electromagn. Res. M*, vol. 110, pp. 119–131, 2022.

[5] E. Çelenk and N. T. Tokan, "Frequency scanning conformal sensor based on SIW metamaterial antenna," *IEEE Sensors J.*, vol. 21, no. 14, pp. 16015–16023, Jul. 2021.

[6] G. Orecchini, M. M. Tentzeris, L. Yang, and L. Roselli, "Smart shoe: An autonomous inkjet-printed RFID system scavenging walking energy," in *Proc. IEEE Int. Symp. Antennas Propag.*, 2011, pp. 1417–1420.

[7] S. Lemey, F. Declercq, and H. Rogier, "Textile antennas as hybrid energy-harvesting platforms," *Proc. IEEE*, vol. 102, no. 11, pp. 1833–1857, Nov. 2014.

[8] X. Lu, P. Wang, D. Niyato, D. I. Kim, and Z. Han, "Wireless networks with RF energy harvesting: A contemporary survey," *IEEE Commun. Surveys Tuts.*, vol. 17, no. 2, pp. 757–789, 2nd Quart. 2015.

[9] G. Akarsu et al., "Development of a novel ultra-wideband textile-based metamaterial absorber for mm-wave band applications," in *Proc. Int. Workshop Antenna Technol.*, 2022, pp. 220–223.

[10] C. C. M. Carmo, R. M. S. Batalha, L. D. Ribeiro, and Ú. C. Resende, "Metamaterial-based broadband absorber design," *IEEE Trans. Magn.*, vol. 58, no. 2, Feb. 2022, Art. no. 2500405.

[11] J. Tak and J. Choi, "A wearable metamaterial microwave absorber," *IEEE Antennas Wireless Propag. Lett.*, vol. 16, pp. 784–787, 2017.

[12] A. Sharma, R. Panwar, and R. Khanna, "Experimental validation of a frequency-selective surface-loaded hybrid metamaterial absorber with wide bandwidth," *IEEE Magn. Lett.*, vol. 10, 2019, Art. no. 2101905.

[13] E. Çelenk and N. T. Tokan, "All-textile, washable metasurface antenna for WBAN/WLAN and mid-band 5G applications," in *Proc. 13th Int. Conf. Elect. Electron. Eng.*, 2021, pp. 305–309.

[14] H. Shielding, "Conductive textile," 4711 datasheet, Revised Dec. 2016. [Online]. Available: https://hollandshielding.com.tr/iletken-tekstil

[15] E. Çelenk and N. T. Tokan, "All-textile on-body antenna for military applications," *IEEE Antennas Wireless Propag. Lett.*, vol. 21, no. 5, pp. 1065–1069, May 2022.

[16] K. Muarrem et al., "Broad band metamaterial absorber based on wheel resonators with lumped elements for microwave energy harvesting," *Opt. Quantum Electron.*, vol. 50, pp. 1–18, 2018.

[17] O. Almirall, R. Fernández-García, and I. Gil, "Wearable metamaterial for electromagnetic radiation shielding," *J. Textile Inst.*, vol. 113, no. 8, pp. 1586–1594, 2022.

[18] M. Yoo, H. K. Kim, S. Kim, M. Tentzeris, and S. Lim, "Silver nanoparticle-based inkjet-printed metamaterial absorber on flexible paper," *IEEE Antennas Wireless Propag. Lett.*, vol. 14, pp. 1718–1721, 2015.

[19] H. Yang, Z. Li, Z. Mei, G. Xiao, H. Deng, and L. Yuan, "Background insensitive polarization-independent ultra-broadband metamaterial perfect absorber in mid-infrared regions," *IEEE Photon. J.*, vol. 14, no. 5, Oct. 2022, Art. no. 2755006.

[20] N. Mishra, D. K. Choudhary, R. Chowdhury, K. Kumari, and R. K. Chaudhary, "An investigation on compact ultra-thin triple band polarization independent metamaterial absorber for microwave frequency applications," *IEEE Access*, vol. 5, pp. 4370–4376, 2017, doi: 10.1109/ACCESS.2017.2675439.

[21] G. Singh, H. Sheokand, K. Chaudhary, K. V. Srivastava, J. Ramkumar, and S. A. Ramakrishna, "Fabrication of a non-wettable wearable textile-based metamaterial microwave absorber," *J. Phys. D: Appl. Phys.*, vol. 52, no. 38, 2019, Art. no. 385304.

[22] E. Erdem and A. H. Yuzer, "Textile-based 3D metamaterial absorber design for X-band application," *Waves Random Complex Media*, pp. 1–10, 2022, doi: 10.1080/17455030.2022.2144655.